# Resonance Raman Studies of Cytochrome P450BM3 and Its Complexes with Exogenous Ligands†

Tian-jing Deng,‡ Leonard M. Proniewicz,‡,§ and James R. Kincaid*,‡

*Department of Chemistry, Marquette University, Milwaukee, Wisconsin 53233, and Chemical Physics Division, Department of Chemistry, and Regional Laboratory of Physicochemical Analysis and Structural Research, Jagiellonian University, Ingardena 3, 30-060 Krakow, Poland*

Hyeyeong Yeom,|| Iain D. G. Macdonald,|| and Stephen G. Sligar*,||

*Beckman Institute for Advanced Science and Technology and Department of Biochemistry, University of Illinois, Urbana, Illinois 61081*

*Received June 7, 1999; Revised Manuscript Received July 30, 1999*

ABSTRACT: Resonance Raman spectra are reported for both the heme domain and holoenzyme of cytochrome P450BM3 in the resting state and for the ferric NO, ferrous CO, and ferrous NO adducts in the absence and presence of the substrate, palmitate. Comparison of the spectrum of the palmitate-bound form of the heme domain with that of the holoenzyme indicates that the presence of the flavin reductase domain alters the structure of the heme domain in such a way that water accessibility to the distal pocket is greater for the holoenzyme, a result that is consistent with analogous studies of cytochrome P450cam. The data for the exogenous ligand adducts are compared to those previously reported for corresponding derivatives of cytochrome P450cam and document significant and important differences for the two proteins. Specifically, while the binding of substrate induces relatively dramatic changes in the $\nu$(Fe−XY) modes of the ferrous CO, ferric NO, and ferrous NO derivatives of cytochrome P450cam, no significant changes are observed for the corresponding derivatives of cytochrome P450BM3 upon binding of palmitate. In fact, the spectral data for substrate-free cytochrome P450BM3 provide evidence for distortion of the Fe−XY fragment, even in the absence of substrate. This apparent distortion, which is nonexistent in the case of substrate-free cytochrome P450cam, is most reasonably attributed to interaction of the Fe−XY fragment with the F87 phenylalanine side chain. This residue is known to lie very close to the heme iron in the substrate-free derivative of cytochrome P450BM3 and has been suggested to prevent hydroxylation of the terminal, $\omega$, position of long-chain fatty acids.

Heme-containing monooxygenases, collectively referred to as cytochromes P450, activate molecular oxygen to generate a potent oxidizing species capable of stereospecific hydroxylation or epoxidation of relatively inert physiological substrates (*1*, *2*). Bacterial cytochrome P450s generally require a three protein system to activate molecular oxygen and are termed class I P450 monooxygenases. Microsomal P450s utilize an NADPH−cytochrome reductase, containing two flavin groups [flavin adenine dinucleotide (FAD) and flavin mononucleotide (FMN)] that sequentially supply low-energy electrons to the (hydroxylating) heme protein. Such two-component protein systems are termed type II monooxygenases (*3*). Liver microsomal enzymes are typically involved in mammalian biochemical pathways and some are implicated in the activation of precarcinogens (*4*). Limited spectroscopic and structural information is available for the eukaryotic class II P450s owing to difficulties in purification/expression and retention of membranous forms at sufficient protein concentrations. Bacterial P450s are soluble, more easily expressed, and more readily purified than their eukaryotic counterparts and hence have been extensively studied by many spectroscopic techniques, and high-resolution crystal structures are available for some in both free and substrate-bound forms (*3*, *5*−*8*).

A soluble bacterial enzyme isolated from *Bacillus megaterium*, designated P450BM3,[1] catalyzes the hydroxylation and epoxidation of long-chain fatty acids such as palmitate and laurate (*9*, *10*). This enzyme is of special interest because, like the mammalian enzymes, it is classified as a type II cytochrome P450, although in this particular case the two component proteins (the heme and reductase domains) are fused together in P450BM3 but may be detached by limited trypsin digestion (*11*) or independently expressed in *Es-*

† This work was supported by grants from the National Institute of Health (DK35153 to J.R.K. and GM33775 and GM31756 to S.G.S.) and is dedicated to our late colleague Hyeyeong Yeom.

* Corresponding authors.

‡ Marquette University.

§ Chemical Physics Division, Department of Chemistry, and Regional Laboratory of Physicochemical Analysis and Structural Research, Jagiellonian University.

|| University of Illinois.

[1] Abbreviations: HBM3, cytochrome P450BM3 holoenzyme; HDBM3, cytochrome P450BM3 heme domain; CAM, cytochrome P450cam; HBM3-O (HDBM3-O), cytochrome P450BM3 holoenzyme (heme domain) at ferric state; HBM3-R (HDBM3-R), cytochrome P450BM3 holoenzyme (heme domain) at ferrous state; HBM3-Op (HDBM3-Op), palmitate-bound ferric cytochrome P450BM3 holoenzyme (heme domain); CAM-Oc, camphor-bound cytochrome P450cam.

10.1021/bi991287j CCC: $18.00 
Published on Web 09/23/1999

*cherichia coli* (*12*). Given its availability and solubility, and its functional similarity to the eukaryotic enzymes, detailed characterization of its structure and function are understandably of great interest.

Of the spectroscopic methods available for characterization of heme protein active sites, resonance Raman (RR) spectroscopy has proven to be highly effective, revealing active-site structural changes in exquisite detail (*13*, *14*). In the case of cytochrome P450cam, in particular, the technique has been used to study very subtle changes in the geometry of bound diatomic ligands induced upon binding of substrate (*15*, *16*), changes that signal direct interaction of the substrate with the Fe−XY fragment. This information is obviously pertinent to the relative stability of the physiologically important dioxygen adducts and the degree of specificity observed in substrate hydroxylation and epoxidation (*17*−*20*).

Herein are reported detailed RR studies of the holoenzyme (in its resting state) and the heme domain of cytochrome P450BM3 in its resting state and for various diatomic ligand adducts: the inherently linear (*14*), isoelectronic ferrous CO and ferric NO species and the inherently bent ferrous NO adduct. Both the stretching and bending modes of the Fe−XY fragment are observed in the RR spectra of the ferrous CO and ferric NO adducts, while only the stretching mode of Fe−XY is observed in the RR spectrum of the ferrous NO adduct. In this case, the vibrational modes of the Fe−XY fragment are insensitive to the binding of substrate.

## MATERIALS AND METHODS

High-copy circular plasmids containing the gene encoding for either the heme domain of P450BM3 (HDBM3) or the holoenzyme under the T7RNA polymerase promoter were expressed as described previously (*21*). Purification of the holoenzyme to an ($A_{418}/A_{280}$) $R_z > 0.6$ has been detailed by Yeom et al. (*21*).

*Expression and Purification of P450BM3 Heme Domain*. The heme domain of P450BM3 was expressed in *E. coli* JM109(DE3). Cells were grown in 2× YT medium, containing ampicillin (100 $\mu$L/mL) at 37 °C for ∼6.5 h at 200 rpm, giving an $OD_{600nm} \approx 1$. Induction was carried out with filter-sterilized 1.0 mM IPTG (isopropyl $\beta$-D-thiogalactopyranoside) at 29 °C and harvested 20 h after induction. Cell paste was stored at −80 °C until further use. Frozen cells were resuspended in the minimum of buffer A (50 mM tris, pH 7.25, 1 mM EDTA, 2 mM dithiothreitol, and 1 mM PMSF) and sonicated on ice (Branson Sonifier 450). Cell debris was removed by centrifugation at 15000*g* for 30 min at 4 °C, keeping the supernatant. DNase and RNase (both 100 $\mu$g/mL) were added to the suspension, which was subsequently stirred at 30 °C for 30 min. A 0−30% ammonium sulfate cut at 4 °C was carried out slowly, the sample was centrifuged at 20000*g* for 15 min, and the resulting supernatant was retained. The 30−60% cut was performed, with the solid fraction retained. This fraction was resuspended in buffer A and dialyzed at 4 °C three consecutive times with a 50-volume excess of buffer A.

The protein extract was loaded onto a DEAE-Sephacel column equilibrated with buffer A at 4 °C. The column was washed with 2 volumes of buffer A at 20 mL/h. Protein was eluted with a 0−500 mM KCl gradient in buffer A at 20 mL/h. Fractions with an $R_z$ $A_{418}/A_{280} > 0.75$ were pooled and concentrated with YM10 membranes. The protein solution was dialyzed three consecutive times with a 50-volume excess of buffer B (25 mM potassium phosphate, pH 6.5, 2 mM DTT, 0.2 mM EDTA, and 1 mM PMSF), and concentrated before being loaded at 4 °C onto a hydroxyapatite (DNA grade, Bio-Rad) column, which was preequilibrated with buffer B. The column was washed with 2 volumes of buffer B before protein was eluted with a gradient of buffer B to buffer C (500 mM potassium phosphate, pH 6.5, 0.2 mM EDTA, 2 mM DTT, and 1 mM PMSF) at a flow rate of 14 mL/h. Fractions with an $R_z >$ 1.50 were pooled, concentrated, and dialyzed 3 × 50-volume excess of buffer A/50% glycerol. SDS−PAGE was performed to confirm protein size and purity. The protein solution was flash-frozen and stored at −80 °C until used for spectroscopic measurements.

Stock solutions of 62 mg/mL (holoenzyme) and 41 mg/mL (heme domain) were available for RR studies. The final concentration for the RR measurements is about 50 $\mu$M. The substrates used in these experiments are a 5 mM stock solution of the sodium salt of palmitic acid in 50 mM $Na_2CO_3$.

*Sample Preparation*. The ferrous CO adduct of P450BM3 heme domain was prepared by adding a small amount of sodium dithionite to a 100 $\mu$L sample of 50 $\mu$M P450BM3 heme domain solution under anaerobic conditions, and bubbling the solution gently with CO for a few minutes. Great care was taken to control the amount of dithionite added, because a large excess can lead to the formation of the P420 CO adduct (*17*). The integrity of the P450BM3 CO adduct was monitored by its UV−vis absorption spectrum. The UV−vis spectrum was taken before and after the Raman experiment to confirm the absence of the P420 form. All RR spectra of the CO adduct in this paper are free of contribution from P420.

The substrate bound P450BM3 heme domain CO adduct was prepared by the addition of a 40-fold molar excess (50 $\mu$L) of the palmitic acid solution to a 25 $\mu$L sample of 200 $\mu$M P450BM3, then phosphate buffer [P100, pH = 7.4] was added to a final volume of 100 $\mu$L and enzyme concentration of 50 $\mu$M. The UV−vis spectrum was measured, monitoring the 390 nm band to confirm the formation of the substrate-bound complex. The CO-bound sample was then prepared in the same manner as described above.

The ferric NO adduct of P450BM3 heme domain (free or substrate-bound) was prepared in the following way: approximately 150 $\mu$L of a 50 $\mu$M P450BM3 heme domain solution, determined by its UV−vis spectrum, was put into a 5 mm NMR tube equipped with a rotationally symmetric valve. The NMR tube was evacuated and backfilled with oxygen-purged argon several times on a vacuum line to remove atmospheric oxygen. Nitric oxide was passed over a column of sodium hydroxide pellets and introduced to the NMR tube via a vacuum line. The final concentration of P450BM3 sample was approximately 50 $\mu$M. It should be noted that extreme care must be taken to remove traces of oxygen from the sample before addition of NO; otherwise protein denaturation occurs.

The preparation of the ferrous NO adduct of P450BM3 heme domain was performed by anaerobic decomposition of sodium nitrite with fresh sodium dithionite (*18*). About 100 $\mu$L of a 50 $\mu$M P450BM3 heme domain sample, either

substrate-bound or free, was placed into a 5 mm NMR tube and sealed with a rubber septum. The sample was vigorously degassed with nitrogen through an inserted syringe needle for several minutes, followed by the injection of about a 100-fold molar excess of sodium dithionite and a 40-fold molar excess of sodium nitrite solution with a gastight syringe. Both of these solutions were also purged with nitrogen prior to injection.

The RR spectra were obtained with a Spex 1269 spectrometer equipped with a Princeton Instruments ICCD-576 UV enhanced detector. The excitation lines employed were the 406.7 nm line from a Spectra-Physics Model 100-K3 krypton ion laser and the 442 nm line from a Liconix Model 4240NB helium−cadmium laser. The spectra were calibrated with fenchone and processed with Spectra-Calc software. A 442 or 413 nm Notch filter (Kaiser Optical) was used to remove the Rayleigh scattered line during the spectral measurement. The NMR tube was spun and a 135° backscattering geometry was employed.

## RESULTS

(*1*) *Ferric P450BM3.* Attempts to document the RR spectra of cytochrome P450BM3 holoenzyme (HBM3) and heme domain (HDBM3) have been previously reported (*22*−*24*). However, in the earlier works employing colloidal silver particles to exploit the SERRS effect, adsorptive surface interactions can apparently alter the enzyme structure, i.e., conversion to the high-spin, five-coordinate state, even in the absence of substrate. While attempts to acquire the RR spectra of both HBM3 and HDBM3, by use of Q-band excitation (∼500 nm), have been reported (*24*), complications arise involving fluorescence from the flavin-containing fused reductase domain and documented photoreduction of the associated heme domain.

In contrast to the earlier works (*22*−*24*), in the soret-excited spectra reported here we observed no evidence for a (HS, 5C) species in the substrate-free forms nor any indication of photoreduction of the heme domain in the spectra of the holoenzyme. The high-frequency RR spectra of HBM3 and HDBM3 are shown in Figure 1 for the substrate-free and palmitate- (p-) bound forms. The overall spectral pattern observed for HDBM3-O is indicative of a hexacoordinated, low-spin state, as expected (*15*). The sixth ligand is a water molecule provided by a cluster of water molecules on the distal side of the heme (*3*). The spectrum of the substrate-free form of the holoenzyme (HBM3-O) shows no significant differences from that of HDBM3-O.

The observed RR frequencies of the palmitate-bound heme domain (HDBM3-Op) document formation of a high-spin, five-coordinate (5C,HS) heme (*13*). However, weak peaks at ∼1502 cm$^{-1}$ ($\nu_3$) and ∼1580 cm$^{-1}$ ($\nu_2$) persist in the RR spectrum of HDBM3-Op, confirming the presence of residual low-spin species in the substrate-bound complex, indicating a low-spin/high-spin equilibrium in the presence of substrate. The persistence of the low-spin form does not reflect incomplete substrate binding, because our experimental conditions (100-fold excess of substrate) and the low $K_d$, 0.02 $\mu$M (*25*), ensure the formation of the paltimate-bound P450BM3 complex. Rather, this behavior is similar to a well-documented manifestation of spin equilibrium within the substrate-bound form in the case of P450cam (*15*, *16*).

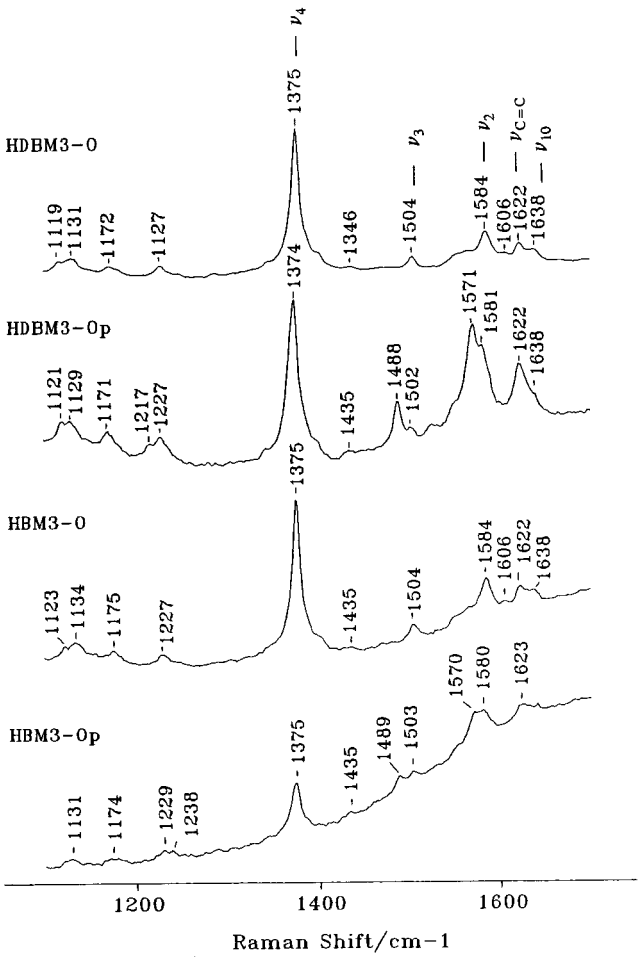


FIGURE 1: High-frequency region (1100−1700 cm$^{-1}$) of RR spectra of P450BM3 heme domain (HDBM3-O), palmitate-bound P450BM3 heme domain (HDBM3-Op), P450BM3 holoenzyme (HBM3-O), and palmitate-bound P450BM3 holoenzyme (HBM3-Op). All spectra were obtained with 406.7 nm excitation with a laser power lower than 20 mW at the sample. For other experimental details see text.

It is important to note that greater 1502/1488 and 1581/1571 intensity ratios observed in the spectrum of HBM3-Op, compared to those in the spectrum of HDBM3-Op, show that the presence of the reductase domain increases the fraction of residual (LS, 6C) component.

Figure 2 presents the low-frequency RR spectra of HBM3-O, HBM3-Op, HDBM3-O, and HDBM3-Op along with those observed for substrate-free (CAM-O) and camphor-bound (CAM-Oc) cytochrome P450cam for comparison. For all the cases (HBM3, HDBM3, and CAM) there is a distinct change in the spectral pattern upon binding of substrates. In the presence of substrate, a new feature appears at 368 cm$^{-1}$ and an apparent intensity increase occurs for a feature near 315 cm$^{-1}$. The other noticeable difference in this set of spectral data is the appearance of an additional feature near 400 cm$^{-1}$ in the spectra of HBM3-O and HDBM3-O that disappears upon binding of palmitate. This feature is missing or only very weakly enhanced in the spectrum of substrate-free P450cam, CAM-O.

According to the most comprehensive set of assignments for low-frequency modes of protoheme (*26*), the in-plane bending modes of the two vinyl substituents appear near 400 and 420 cm$^{-1}$. In-plane deformation modes of the heme macrocycle appear near 345 cm$^{-1}$ ($\nu_8$), ∼270 cm$^{-1}$ ($\nu_{52}$),

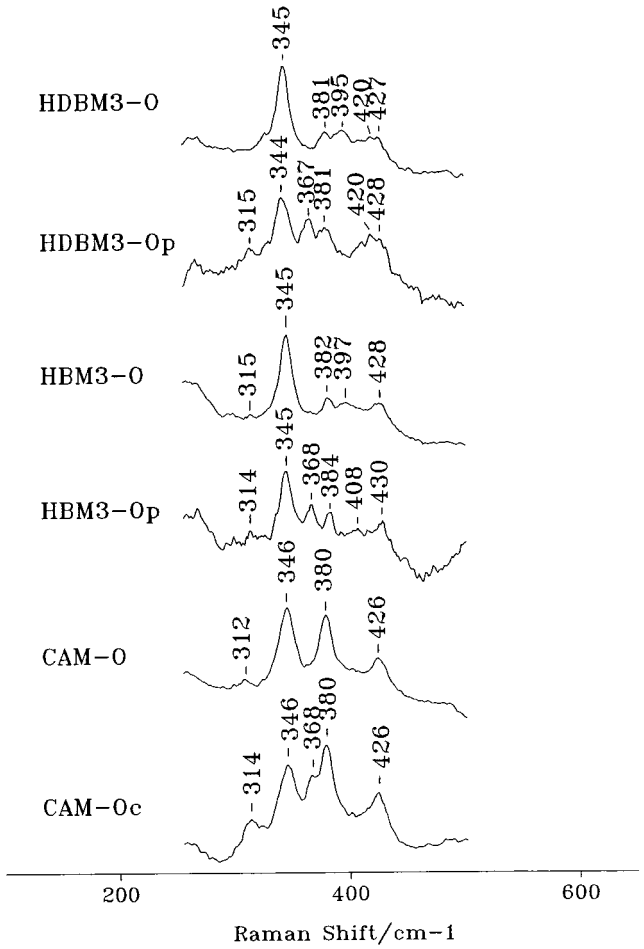


FIGURE 2: Low-frequency region (250−500 $cm^{-1}$) of RR spectra of P450BM3 heme domain (HDBM3-O), palmitate-bound P450BM3 heme domain (HDBM3-Op), P450BM3 holoenzyme (HBM3-O), palmitate-bound P450BM3 holoenzyme (HBM3-Op), P450cam (CAM-O), and camphor-bound P450cam (CAM-Oc). P450cam was produced according to a previously reported method (*15*). All spectra were obtained with 406.7 nm excitation with a laser power lower than 20 mW at the sample. For other experimental details see text.

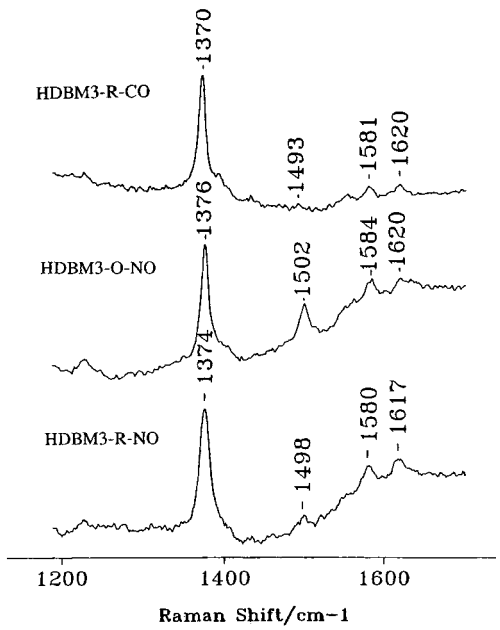


FIGURE 3: High-frequency region (1200−1700 $cm^{-1}$) of RR spectra of CO adduct of ferrous P450BM3 heme domain (HDBM3-R−CO), NO adduct of ferric P450BM3 heme domain (HDBM3-O−NO), and NO adduct of ferrous P450BM3 heme domain (HDBM3-R−NO). All spectra were obtained with 442 nm excitation with a laser power lower than 15 mW at the sample. For other experimental details see text.

and 250 $cm^{-1}$ ($\nu_9$), while the relatively strong feature appearing near 380 $cm^{-1}$ is attributed to a mode containing substantial involvement of propionate deformation. Upon conversion to the high-spin state, in this situation induced by substrate binding, out-of-plane deformations are activated. In the present cases, the feature near 367 $cm^{-1}$ is essentially absent in the substrate-free derivatives but appears as one of the strongest features for the corresponding substrate-bound species. Second, the weak feature observed near 315 $cm^{-1}$ in the substrate-free derivatives appears to grow in intensity upon substrate binding. The most reasonable assignments of these two features are to $\gamma_6$ and $\gamma_7$, respectively (*26*). However, this remains to be confirmed by a study of these proteins reconstituted with *meso*-deuterated protoheme; i.e., both $\gamma_6$ and $\gamma_7$ are known to experience rather large shifts upon meso-deuteration (*26*).

In addition to the in-plane and out-of-plane deformations of the macrocycle core and its peripheral groups, the stretching mode of the Fe−S linkage to the proximal cysteine ligand is expected to occur in this spectral region. It is observed at 351 $cm^{-1}$ in the spectrum of the high-spin, substrate-bound derivative of cytochrome P450cam, being enhanced only with excitation near 350 nm, and is not observed in the spectrum of the low-spin substrate-free species (*15*, *16*, *27*). Similar behavior and an identical frequency for substrate-bound HDBM3 has been observed (I. D. G. Macdonald, unpublished data).

(*2*) *Ferrous CO Complex of P450BM3.* The high-frequency (1200−1700 $cm^{-1}$) RR spectrum of the ferrous CO adduct of HDBM3 (HDBM3-R−CO) is displayed in Figure 3. The $\nu_4$, $\nu_3$, and $\nu_2$ modes occur at 1370, 1493, and 1581 $cm^{-1}$, respectively. No evidence of a band at 1345 $cm^{-1}$, which is the marker band of iron(II) heme, is detected, eliminating the possibility of spectral contamination by a photodissociated reduced (deligated) product (*17*). Figure 4 presents the low-frequency region (200−800 $cm^{-1}$) of the RR spectra of the natural abundance and isotopically labeled analogues of the ferrous CO adduct of HDBM3 (HDBM3-R−$^{12}$CO and HDBM3-R−$^{13}$CO). A strong peak at 471 $cm^{-1}$ shifts to 468 $cm^{-1}$ and a weak peak at 558 $cm^{-1}$ shifts to 544 $cm^{-1}$ upon $^{13}$CO substitution. Quite similar isotopic shifts have been observed (*28*) and calculated (*29*) for the ferrous CO adduct of P450cam, thus supporting the assignment of the 471 $cm^{-1}$ feature to $\nu$(Fe−CO) and the 558 $cm^{-1}$ feature to $\delta$(Fe−CO).

The RR spectrum of the palmitate-bound CO adduct of P450BM3 heme domain (HDBM3-Rp−CO) is shown in Figure 4. We note that addition of substrate either before or after the introduction of CO yields identical RR and UV−vis spectra. Interestingly, there are no obvious spectroscopic changes observed in the low-frequency region upon substrate binding, a result in direct contrast with the behavior of P450cam, whereupon binding of substrate induced a shift of $\nu$(Fe−CO) from 464 to 484 $cm^{-1}$ (*16*, *28*).

(*3*) *Nitrosyl Adduct of Ferric P450BM3.* The high-frequency region of the RR spectrum of the ferric NO adduct of

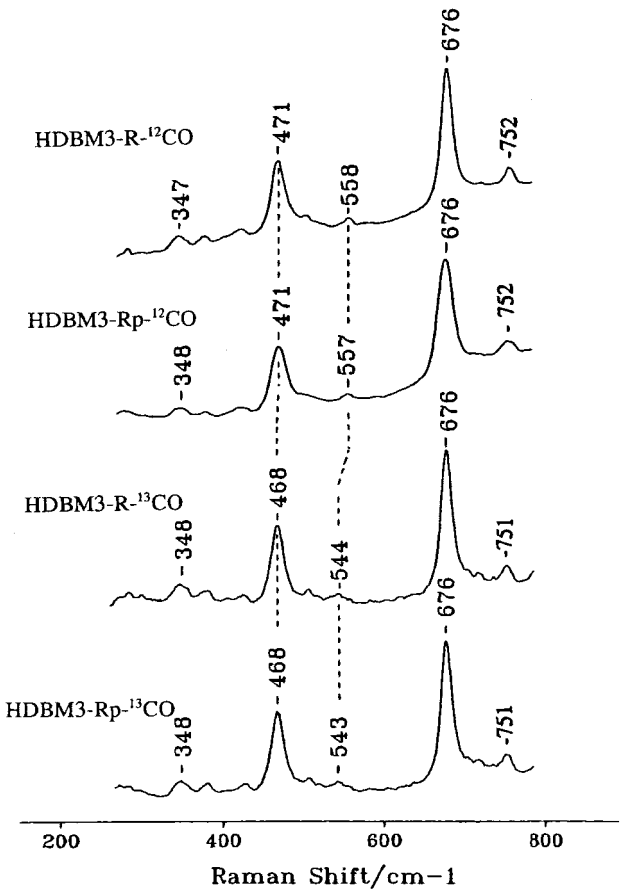


FIGURE 4: RR spectra of CO adducts of ferrous P450BM3 heme domain: $^{12}CO$, substrate-free (HDBM3-R−$^{12}CO$); $^{12}CO$, palmitate-bound (HDBM3-Rp-$^{12}CO$); $^{13}CO$, substrate-free (HDBM3-R−$^{13}CO$); and $^{13}CO$, palmitate-bound (HDBM3-Rp−$^{13}CO$). All spectra were obtained with 442 nm excitation with a laser power less than 15 mW at the sample. For other experimental details see text.

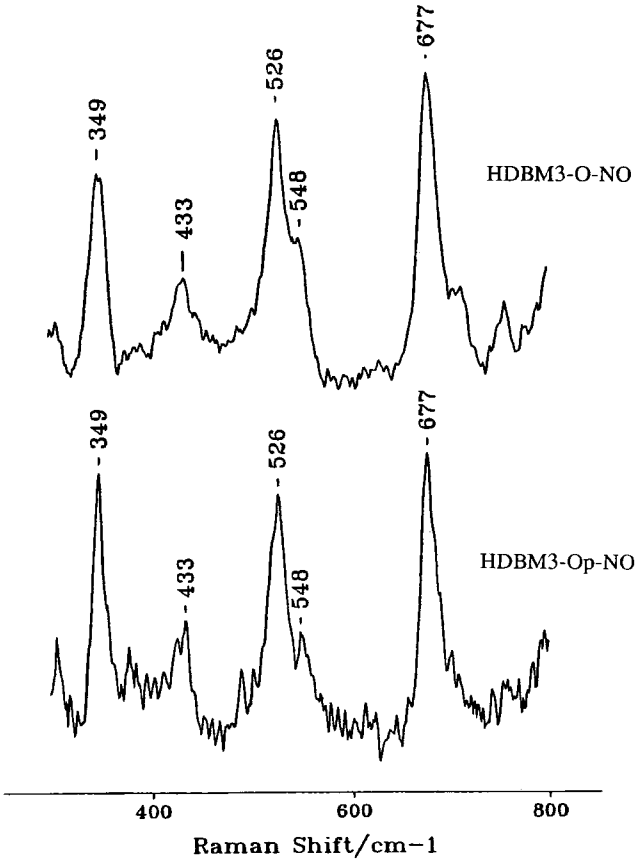


FIGURE 5: RR spectra of NO adducts of ferric P450BM3 heme domain: substrate-free (HDBM3-O−NO) and palmitate-bound (HDBM3-Op−NO). All spectra were obtained with 442 nm excitation with a laser power less than 15 mW at the sample. For other experimental details see text.

HDBM3 (HDBM3-O−NO) is displayed in Figure 3. The $\nu_2$, $\nu_3$, and $\nu_4$ modes, which are sensitive to the oxidation state and spin state change, are used to check for possible autoreduction of $Fe^{III}$−NO (*17*). As shown in the spectrum, the position of these three modes (1584 $cm^{-1}$ for $\nu_3$, 1502 $cm^{-1}$ for $\nu_2$, and 1376 $cm^{-1}$ for $\nu_4$) indicates hexacoordinated, low-spin ferric heme iron. There is no 1345 $cm^{-1}$ feature detected in the spectrum of the ferric NO adduct, eliminating possible spectral contamination by the deligated autoreduced species.

Figure 5 presents the low-frequency (300−800 $cm^{-1}$) RR spectrum of the NO adduct of ferric P450BM3 (HDBM3-O−NO). The bands at 349 and 677 $cm^{-1}$ are assigned to the $\nu_8$ and $\nu_7$ modes of the heme skeleton (*15*). There are two bands located in the low-frequency region besides the heme skeletal modes. One exhibits intensity comparable to $\nu_7$ and occurs at 526 $cm^{-1}$, while the other band of lower intensity is positioned at 548 $cm^{-1}$. By comparison with the ferric P450cam NO adduct (*17*), the 526 $cm^{-1}$ band is assigned here to the stretching mode of Fe(III)−NO and the 548 $cm^{-1}$ feature to the corresponding bending mode, $\delta$(FeNO). The enhancement of the latter suggests a somewhat distorted Fe−NO linkage as has been previously documented for camphor-bound P450cam (*17*). The RR spectrum of the ferric NO adduct of HDBM3 in the presence of palmitate (HDBM3-Op−NO) is also shown in Figure 5. Clearly, the binding of palmitate appears to have an insignificant effect on the Fe−NO linkage in P450BM3. In brief, the results of RR spectral studies of the ferric NO adduct are consistent with the result for the CO adduct of ferrous P450BM3. Namely, a slightly distorted Fe−XY linkage exists in HDBM3, unlike the corresponding CAM-R−CO and CAM-O−NO, and shows minimal sensitivity to the presence of substrate.

(*4*) *Ferrous Nitrosyl Adduct of P450BM3.* Figure 3 displays the high-frequency region (1200−1700 $cm^{-1}$) of the RR spectrum of the ferrous NO P450BM3 adduct (HDBM3-R−NO). The $\nu_3$ and $\nu_2$ peaks occur at 1498 and 1580 $cm^{-1}$, respectively, indicating low-spin, hexacoordinated heme iron. Any possible spectral contamination from a deligated ferrous adduct is eliminated by the absence of a 1345 $cm^{-1}$ peak.

The low-frequency RR spectra of the ferrous NO adducts of P450BM3 (HDBM3-R−$^{14}$NO) are displayed in Figure 6. The band located at 543 $cm^{-1}$ is clearly associated with bound NO as it displays isotopic sensitivity, shifting to 529 $cm^{-1}$ upon substitution with $^{15}$NO (HDBM3-R−$^{15}$NO). No other obvious isotope-sensitive feature is observed in the low-frequency region of the spectrum.

Consistent with earlier studies of the ferrous NO adduct of P450cam (*18*), the 544 $cm^{-1}$ band in the RR spectrum of HDBM3-R−NO adduct observed here is assigned as the $\nu(Fe^{II}$−NO). In the present study, the $\delta(Fe^{II}$−NO) mode is not easily detected in the region where it is expected [~440 $cm^{-1}$] owing to the complicated spectral pattern caused by overlapping porphyrin modes and the relatively low spectral signal-to-noise ratio.

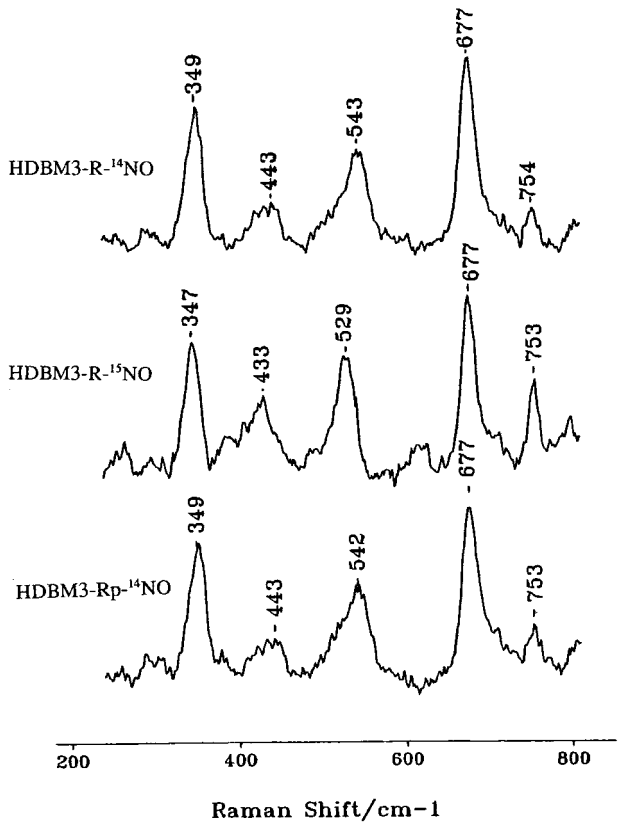


FIGURE 6: RR spectra of NO adducts of ferrous P450BM3 heme domain: $^{14}$NO, substrate-free (HDBM3-R−$^{14}$NO); $^{15}$NO, substrate-free (HDBM3-R−$^{15}$NO); and $^{14}$NO, palmitate-bound (HDBM3-Rp−$^{14}$NO). All spectra were obtained with 442 nm excitation with a laser power lower than 15 mW at the sample. For other experimental details see text.

Figure 6 also presents the RR spectrum of the palmitate-bound ferrous NO adduct of P450BM3 (HDBM3-Rp−$^{14}$NO). The spectrum exhibits no obvious differences from that of the substrate-free adduct, indicating that binding of substrate has no significant effect on the Fe(II)−NO fragment.

## DISCUSSION

(*A*) *Resting State*. As can be seen in Figure 1, the binding of substrate to these cytochromes P450 induces readily detectable changes in the RR spectra that are indicative of a conversion from a (LS, 6C) state to a (HS, 5C) state; i.e., $\nu_3$ and $\nu_2$ shift down. The spin and coordination number alteration is the result of displacement of the aqueous ligand upon the binding of the substrate, converting the heme iron to a (HS, 5C) state. Substrate binding has been shown to control/regulate electron delivery to the heme iron by increasing its redox potential, facilitating its reduction (*30*, *31*). In the case of P450BM3, the persistence of residual intensities at 1502 and 1580 cm$^{-1}$ supports the existence of an equilibrium between the low- and high-spin forms in the presence of substrate. Such an equilibrium has been previously reported for substrate-bound P450cam (*15*, *16*):

$$\text{S·P450 (HS, 5C)} + \text{H}_2\text{O} \rightleftarrows \text{S·P450·H}_2\text{O (LS, 6C)} \quad (1)$$

In the latter case, the percentage of residual low-spin component has been shown to be dependent on substrate structure, with the natural substrate camphor and its close structural analogue, admantanone, yielding (HS, 5C) fractions of 97% and 99%, respectively. With smaller substrates, a greater fraction of (LS, 6C) complexes are observed; e.g., for norcamphor the fraction of (HS, 5C) is only 46% (*32*).

Comparisons of the spectra obtained for HDBM3-O and HDBM3-Op with those obtained for HBM3-O and HBM3-Op does reveal an important difference. Thus, the presence of the fused reductase domain in HBM3-Op results in a larger amount of residual (LS, 6C) species, compared to that observed for HDBM3-Op; i.e., the 1581/1571 and 1502/1488 ratios are greater for HBM3-Op. This effect is directly analogous to similar behavior observed for cytochrome P450cam upon interaction with its redox partner, putidaredoxin (Pd), wherein it was shown that the percentage of (HS, 5C) component diminishes upon binding of Pd to the camphor-bound form (*33*). This increase in the amount of residual (LS, 6C) component is most reasonably attributable to slight changes in the architecture of these enzymes upon binding of the redox partner, changes that evidently permit retention of additional water molecules in the distal pocket.

(*B*) *Exogenous Ligand Adducts*. (*1*) *Factors That Determine the Frequencies of the Fe*−*XY Fragment*. The inherent geometry (i.e., linear or bent) of the M−XY fragment of diatomic ligand adducts of metalloporphyrins or heme proteins depends on the total number of electrons in the iron d$\pi$ and ligand $\pi$* orbitals (*14*). The M−XY fragment changes from linear to bent when the number of electrons in these orbitals increases from 6 to 7 or more. Considering the case of interest here, the total electron count of six in the Fe(II)−CO and Fe(III)−NO adducts favors an essentially linear geometry, while the seven electron count in the case of the Fe(II)−NO adducts predicts an inherently bent geometry.

Resonance Raman spectroscopy has been proven to be an especially effective probe of the M−XY geometry (*14*, *29*). In the absence of any off-axis interactions that effectively lower the symmetry, the bending mode is theoretically not active in the RR spectrum. Thus, appearance of the $\delta$(M−XY) mode in the RR can be taken as a reliable indicator of some type of off-axis interaction, with symmetry lowering being effectively induced by steric factors, hydrogen bonding, and/or some type of polar influence (*29*, *34*).

(*2*) *Comparison between P450BM3 and P450cam*. The RR spectral studies of cytochrome P450cam, the most-studied cytochrome P450, provide a useful starting point for the investigation of substrate-binding effects on the iron−ligand fragment. Detailed RR studies of the CO, NO, and CN$^-$ adducts of P450cam have been carried out in recent years (*16*−*20*, *28*). To achieve a better understanding of the substrate-binding effects on the Fe−XY fragment in the active site of P450BM3, it is useful to compare the present results to the corresponding data for P450cam.

Cytochrome P450cam and P450BM3 are both b-type heme proteins, with a cysteine ligand on the proximal side of the heme. The RR spectra of substrate-free P450cam and P450BM3 are almost identical, in both the low- and high-frequency regions. The Fe−S$^-$ stretching frequency of the high-spin, substrate-bound species is identical in both proteins (I. D. G. Macdonald, unpublished data), suggesting minimal structural or bonding differences between the proteins in terms of the *proximal* ligand environment. The difference in vibrational signatures of the Fe−XY fragment between

these two ligand-bound proteins is therefore most reasonably attributed to differences within the *distal* heme environment.

(*a*) *Inherently Linear Fe(II)−CO and Fe(III)−NO Adducts*. The $\nu$(Fe−CO) of the substrate-free form of the ferrous CO adduct of P450cam is located at 464 cm$^{-1}$ and the $\delta$(Fe−CO) mode is not observed (*16*, *28*). The $\nu$(Fe−CO) is found to be influenced by the size of the substrate, being observed at 473 cm$^{-1}$ when the small size substrate, norcamphor, is bound and at 484 cm$^{-1}$ when a larger substrate (e.g., camphor) is bound to P450cam (*28*). The bending mode, which occurs at 558 cm$^{-1}$, is also observed in the substrate-bound form. The X-ray structure of carbon monoxide-ligated, camphor-bound P450cam reveals a 168° bending angle for the Fe−C−O linkage (*35*). These spectroscopic and structural observations suggest that the Fe−CO linkage is essentially linear in the absence of substrate and that steric hindrance, induced by the substrate, perturbs the Fe−CO fragment to bend away from its normal 180° geometry, suggesting it is the size of the substrate that alters the apparent bending angle ($\theta$) of the Fe−C−O linkage. This distortion activates the $\delta$(Fe−CO) bending mode and also causes an increase in frequency of the $\nu$(Fe−CO) stretching mode, owing to the influence of kinematic coupling effects that counteract the expected weakening in the $\pi$-back-bonding (*14*, *34*). In fact, recent DFT calculations conducted by Ghosh and Bocian (*36*) as well as others (*37*, *38*), have revealed a surprisingly large stretch/bend interaction force constant that has important implications for predicted energy requirements for Fe−CO distortion and also accounts for the observed increase in $\nu$(Fe−CO) upon distortion.

The vibrational behavior of the Fe−NO fragment in the isoelectronic Fe$^{III}$−NO adduct is entirely consistent with the data for the Fe$^{II}$−CO adduct. Thus, as discussed in a previous work involving NO adducts of ferric P450cam (*17*), as the substrate size increased, the $\delta$(FeNO) bending mode is activated and the $\nu$(Fe−NO) shifts to lower frequency, a trend opposite to that found for the ferrous CO adducts, where shifts to high frequency were observed. The reasons for this opposite trend in shifts of $\nu$(Fe−NO) and $\nu$(Fe−CO) have been discussed previously (*17*, *39*).

In direct contrast to the P450cam protein, the ferrous CO adduct of P450BM3 exhibits both stretching and bending modes in the substrate-free state (Figure 4). Also, substrate-binding has no obvious effect on the Fe−CO linkage in contrast to that observed for P450cam. The frequency of the $\delta$(Fe−CO) is almost identical to the $\delta$(Fe−CO) of camphor-bound P450cam, and the $\nu$(Fe−CO) (473 cm$^{-1}$) lies between that of substrate-free P450cam (464 cm$^{-1}$) and that of camphor-bound P450cam (484 cm$^{-1}$). Thus, even in the absence of substrate, the inherently linear Fe−CO fragment is distorted in the case of P450BM3.

Consistent with the data for Fe$^{II}$−CO adduct, both $\nu$(Fe$^{III}$−NO), 526 cm$^{-1}$, and $\delta$(Fe$^{III}$−NO), 548 cm$^{-1}$, are observed in the RR spectrum of the substrate-free ferric P450BM3 NO adduct. As in the case of the CO adduct, the frequency of the $\nu$(Fe$^{III}$−NO) lies between that of substrate-free P450cam (528 cm$^{-1}$) and that of camphor-bound P450cam (522 cm$^{-1}$). Again, substrate binding has no significant effect on the RR spectra of the ferric NO adduct of P450BM3.

(*b*) *Inherently Bent Fe$^{II}$−NO Adduct*. The inherently bent Fe$^{II}$−NO linkage exhibits both stretching and bending modes in the RR spectrum of the nitric oxide adduct of ferrous P450cam (*18*). The $\nu$(Fe$^{II}$−NO) band, occurring at 547 cm$^{-1}$ in the absence of substrate, shifts to 554 cm$^{-1}$ upon the binding of larger substrates, adamantanone and camphor. The $\delta$(Fe$^{II}$−NO) shows only 1 or 2 cm$^{-1}$ variation upon substrate binding. Not surprisingly, a smaller substrate, norcamphor, exhibits no observed effect on $\nu$(Fe$^{II}$−NO). This observation is in contrast with the results obtained from the RR spectra of the inherently linear ferrous CO (*16*) and ferric NO adducts (*17*), in which norcamphor induces significant shifts of $\nu$(Fe$^{II}$−CO) and $\nu$(Fe$^{III}$−NO). Inasmuch as the Fe$^{II}$NO fragment of the P450cam is inherently bent, further steric strain is imposed only by larger substrates, camphor and adamantanone.

The $\nu$(Fe$^{II}$−NO) in ferrous P450BM3 NO adduct (544 cm$^{-1}$) is close to that of P450cam (547 cm$^{-1}$ ). The binding of long-chain fatty acids has no significant effects on $\nu$(Fe$^{II}$−NO). This observation is consistent with the data from Fe$^{II}$−CO and Fe$^{II}$−NO, which are discussed above. The absence of a substrate-binding effect on $\nu$(Fe$^{II}$−NO) in the case of P450BM3 is certainly not surprising, considering the fact that substrate binding showed no influence even in the case of the inherently linear Fe−XY fragments in the ferric NO and ferrous CO adducts of P450BM3.

(*C*) *Functional Relevance*. In the case of P450cam, Sligar and co-workers (*31*, *32*, *40*) found that the percentage of the high- and low-spin species depends on the mobility of the substrate, with more highly mobile substrates leading to a high percentage of ligated form. Therefore, the mixture of two types of spin species in substrate-bound P450BM3 suggests that highly flexible long-chain acids allow some water molecules to remain present in the heme pocket. Furthermore, NMR paramagnetic relaxation studies (*41*), as well as the recently available structure of a substrate-bound P450BM3 complex (*8*), show that there is sufficient space for a water molecule to reside.

The apparent differences in the Fe−XY geometry between P450cam and P450BM3 XY adducts are directly relevant to observed differences in substrate binding and enzyme activity. The essentially linear Fe−CO and ferric Fe−NO fragments of substrate-free P450cam are distorted upon binding substrate, an observation that is consistent with the fact that in cytochrome P450cam the substrate is rigidly held in a precise orientation that accounts for exclusive hydroxylation of a single site on the natural substrate, camphor. On the other hand, the hydroxylation of the long-chain fatty acids by P450BM3 takes place at $\omega$-1, $\omega$-2, and $\omega$-3 positions depending on the length of the fatty acid chain (*42*, *43*). Yet, in contrast to the mammalian P450s, which efficiently hydroxylate the terminal ($\omega$) position of fatty acids, P450BM3 does not catalyze terminal hydroxylation. It cannot be the lower reactivity of the $\omega$ position, relative to that of the secondary carbons, that accounts for this lack of reactivity, because fatty acids bearing a terminal (inherently more reactive) double bond are hydroxylated only at the $\omega$-2 position with little evidence for reaction at the unsaturated position (*44*).

Significantly, the X-ray crystal structure investigations (*3*, *8*) reveal the fact that the F87 residue of P450BM3 lies quite close to the heme macrocycle, apparently "sequestering" the terminal position from attack (*3*, *8*). Support for this proposal is provided by recent studies of the specificity of the F87A mutant of P450BM3 by Modi and co-workers (*45*), wherein

it is observed that replacement of the F87 residue with the smaller alanine converts the enzyme to an efficient $\omega$-hydroxylase.

The RR results reported here are entirely consistent with these proposals. Thus, in the case of the Fe−XY adducts of P450BM3, even in the absence of substrate, the RR data clearly document a distortion in the inherently linear $Fe^{II}$−CO and $Fe^{III}$−NO fragments; a distortion that is most reasonably attributed to the steric hindrance imposed by the F87 residue. Clearly, future studies of the RR spectra of mutant proteins, especially the F87A mutant studied by Modi and co-workers (*45*), would be useful to test this hypothesis.

## REFERENCES


1. Gunsalus, I. C., Meek, J. R., Lipscomb, J. D., Debrunner, P., and Munk, E. (1974) in *Molecular Mechanism of Oxygen Activation* (Hayashi, O., Ed.), p 559, Academic Press, New York.
2. White, R. E., and Coon, M. J. (1980) *Annu. Rev. Biochem. 49*, 315.
3. Ravichandran, K. G., Boddupalli, S. S., Hasemann, C. A., Peterson, J. A., and Deisenhofer. J., (1993) *Science 261*, 731.
4. Coon, M. J., and Koop, D. R., (1983) *Enzyme 16*, 645.
5. Poulos, T. L., Finzel, B. C. and Howard, A. J. (1987) *J. Mol. Biol. 195*, 731.
6. Cupp-Vickery, J. R. and Poulos, T. L. (1995) *Nat. Struct. Biol. 2*, 144.
7. Hasemann, C. A., Ravichandran, K. G., Peterson, J. A., and Deisenhofer, J. (1994) *J. Mol. Biol. 236*, 1169.
8. Li, H. and Poulos, T. L., (1997) *Nat. Struct. Biol. 4*, 140.
9. Ho, P. P., and Fulco, A. J., (1976) *Biochim. Biophys. Acta 431*, 246.
10. Ruettinger, R. T., and Fulco, A. J., (1981) *J. Biol. Chem. 256*, 5728.
11. Narhi, L. O., and Fulco, A. J. (1987) *J. Biol. Chem. 262*, 6683.
12. Boddupalli, S. S., Pramanik, B. C., Slaughter, C. A., Estabrook, R. W., and Peterson, J. A. (1992) *Arch. Biochem. Biophys. 292*, 20.
13. Spiro, T. G., Ed. (1988) *Biological Application of Raman Spectroscopy*, Vol. 3, John Wiley & Sons, New York.
14. Yu, N.-T. (1986) *Methods in Enzymology*, Vol. 130, p 350, Academic Press, New York.
15. Champion, P. M., Gunsalus, I. C., and Wagner, G. C. (1978) *J. Am. Chem. Soc. 100*, 3743.
16. Wells, A. V., Li, P., Champion, P. M., Martinis, S. A., and Sligar, S. G (1992) *Biochemistry 31*, 4384.
17. Hu, S., and Kincaid, J. R. (1991) *J. Am. Chem. Soc. 113*, 2843.
18. Hu, S., and Kincaid, J. R. (1991) *J. Am. Chem. Soc. 113*, 9760.
19. Simianu, M. C., and Kincaid, J. R. (1995) *J. Am. Chem. Soc. 117*, 4638.
20. Hu, S., Schneider, A. J., and Kincaid, J. R. (1991) *J. Am. Chem. Soc. 113*, 4815.
21. Yeom, H., Sligar, S. G., Li, H., Poulos, T. L., and Fulco, A. J. (1995) *Biochemistry 34*, 14733.
22. Macdonald, I., Munro, A. W., and Smith, W. E. (1998) *Biophys. J. 74*, 3241.
23. Miles, J. R., Munro, A. W., Rospendowski, B. N., Smith, W. E, McKnight, J., and Thomson, A. J. (1992) *J. Biochem. 288*, 503.
24. Hudecek, J., Baumruk, V., Anzenbacher, P., and Munro, A. W. (1998) *Biochem. Biophys. Res. Commun. 148*, 811.
25. Maves, S. A., Yeom, H., McLean, M. A., and Sligar, S. G., (1997) *FEBS Lett. 414*, 213.
26. Hu, S., Smith, K. M., and Spiro, T. G. (1996) *J. Am. Chem. Soc. 118*, 12638.
27. Champion, P. M., Stallard, B. R., Wagner, G. C., and Gunsalus, I. C. (1982) *J. Am. Chem. Soc. 104*, 5469.
28. Uno, T., Nishimura, Y., Nakino, R., Lizuka, T., Ishimura, Y., and Tsuboi, M. (1985) *J. Biol. Chem. 260*, 2023.
29. Li, X. Y., and Spiro, T. G. (1988) *J. Am. Chem. Soc. 110*, 6024.
30. Sligar, S. G., and Gunsalus, I. C. (1976) *Proc. Natl. Acad. Sci. U.S.A. 73*, 1078.
31. Fisher, M. T., and Sligar, S. G. (1983) *J. Am. Chem. Soc. 107*, 5018.
32. Fisher, M. T., and Sligar, S. G. (1985) *Biochemistry 24*, 6696.
33. Unno, M., Christian, J. F., Benson, D. E., Gerber, N. C., Sligar, S. G., and Champion, P. M. (1997) *J. Am. Chem. Soc. 119*, 6614.
34. Ray, G. B., Li, X.-Y., Ibers, J. A., Sessler, J. L., and Spiro, T. G. (1994) *J. Am. Chem. Soc. 116*, 162.
35. Raag, R., and Poulos, T. L. (1989) *Biochemistry 28*, 7586.
36. Ghosh, A., and Bocian, D. F. (1996) *J. Phys. Chem. 100*, 6363.
37. Kozlowski, P. M., Rush, T. S., III, Jarzecki, A. A., Zgierski, M. Z., Chase, B., Piffat, C., Ye, B.-H., Li, X.-Y., Pulay, P., and Spiro, T. G. (1999) *J. Phys. Chem. A 103*, 1357.
38. Papai, I., Stirling, A., Mink, J., and Nakamoto, K. (1998) *Chem. Phys. Lett. 287*, 531.
39. Wang, J., Caughey, W. S., and Rousseau, D. C. (1996) in *Methods in Nitric Oxide Research* (Feelisch, M., and Stamler, J. S., Eds.) John Wiley & Sons, New York.
40. Whit, R. E., McCarthy, M.-B., Egeberg, K. D., and Sligar, S. G. (1984) *Arch. Biochem. Biophys. 228*, 493.
41. Modi, S., Primrose, W. U., Boyle, J. M. B., Gibson, C. F., Lian, L.-Y., and Robert, G. C. K. (1995) *Biochemistry 34*, 8982.
42. Narhi, L. O., and Fulco, A. J., (1986) *J. Biol. Chem. 261*, 7160.
43. Boddupalli, S. S., Estabrook, R. W., and Peterson, J. A. (1990) *J. Mol. Biol. 265*, 4233.
44. Shirane, N., Sui, Z., Peterson, J. A., and Ortiz de Montellano, P. R. (1993) *Biochemistry 32*, 13732.
45. Oliver, F. C., Modi, S., Sutcliffe, M. J., Primrose, W. U., Lian, L.-Y., and Robert, G. C. K. (1997) *Biochemistry 36*, 1567.


BI991287J